Cerebral Cortex, January 2016;26: 384–401

doi: 10.1093/cercor/bhu294
Advance Access Publication Date: 9 December 2014
Original Article

ORIGINAL ARTICLE

The Effect of Task Instruction on Haptic Texture Processing: The Neural Underpinning of Roughness and Spatial Density Perception

Judith Eck[1,2], Amanda L. Kaas[1], Joost L. Mulders[2], Lars Hausfeld[1], Zoe Kourtzi[3], and Rainer Goebel[1,2,4]

[1]Department of Cognitive Neuroscience, Maastricht University, The Netherlands, [2]Brain Innovation B.V., Maastricht, The Netherlands, [3]Department of Psychology, University of Cambridge, Cambridge, UK, and [4]Netherlands Institute for Neuroscience, Institute of the Royal Netherlands Academy of Arts and Sciences (KNAW), Amsterdam, The Netherlands

Address correspondence to Judith Eck, Department of Cognitive Neuroscience, Maastricht University, Oxfordlaan 55, 6229 EV Maastricht, The Netherlands. Email: judith.eck@maastrichtuniversity.nl

Abstract

Perceived roughness is associated with a variety of physical factors and multiple peripheral afferent types. The current study investigated whether this complexity of the mapping between physical and perceptual space is reflected at the cortical level. In an integrative psychophysical and imaging approach, we used dot pattern stimuli for which previous studies reported a simple linear relationship of interdot spacing and perceived spatial density and a more complex function of perceived roughness. Thus, by using both a roughness and a spatial estimation task, the physical and perceived stimulus characteristics could be dissociated, with the spatial density task controlling for the processing of low-level sensory aspects. Multivoxel pattern analysis was used to investigate which brain regions hold information indicative of the level of the perceived texture characteristics. While information about differences in perceived roughness was primarily available in higher-order cortices, that is, the operculo-insular cortex and a ventral visual cortex region, information about perceived spatial density could already be derived from early somatosensory and visual regions. This result indicates that cortical processing reflects the different complexities of the evaluated haptic texture dimensions. Furthermore, this study is to our knowledge the first to show a contribution of the visual cortex to tactile roughness perception.

Key words: roughness, somatosensory cortex, spatial density, tactile, visual cortex

Introduction

The way we interact with objects in our environment is partly determined by material properties such as texture. Texture is a multidimensional construct and can be described by several perceptual attributes such as rough, dense, soft, slippery, and thick (Lederman et al. 1986; Hollins et al. 1993, 2000; Picard et al. 2003; Gescheider et al. 2005; Bergmann Tiest and Kappers 2006).

For roughness, the mapping between physical and perceptual space has extensively been studied. Physical roughness can be described as being associated with several physical stimulus properties, including height differences, spatial properties of the texture (e.g., the spacing between single texture elements), and friction (Bergmann Tiest 2010). The effect of these factors on perceived surface roughness has been investigated and confirmed in numerous studies (Lederman and Taylor 1972; Blake

et al. 1997; Bergmann Tiest and Kappers 2007), in particular for coarse textures like gratings and dot pattern textures (Connor et al. 1990; Meftah et al. 2000; Merabet et al. 2004; Gescheider et al. 2005; Lawrence et al. 2007; Dépeault et al. 2009). Hence, roughness perception is very likely influenced by a combination of different physical factors.

The complexity of the mapping of the physical stimulus space to perceptual space also appears to be reflected in the neural coding in the periphery. Roughness perception was recently shown to be mediated by multiple mechanoafferents, that is, the rapidly adapting (RA) and Pacinian (PC) afferents as well as the slowly adapting type I cutaneous afferents (SA1) (Weber et al. 2013). Although the spatial code conveyed by SA1 appears to be dominant for coarse textures, such as dot pattern textures, the combined use of SA1 spatial variation as well as RA and PC temporal variation result in an improved prediction for perceived roughness (Weber et al. 2013). Hence again, roughness can only be represented using a combination of different afferent channels.

The outstanding question is whether and how the complexity of the mapping of the physical stimulus space to perceptual space affects cortical processing. What is the contribution of different cortical regions to the perception of different texture dimensions, and what kind of perceptual representation do they contain?

Most previous studies on haptic texture processing do not allow inferences regarding this question, because they do not dissociate the physical stimulus characteristics from the perceived texture dimensions. They do, however, provide important insights in the cortical network involved in haptic texture perception in general. Next to activation clusters in the postcentral gyrus (PoCG)—presumably the primary somatosensory cortex (S1; Deshpande et al. 2008; Stilla and Sathian 2008; Sathian et al. 2011)—studies on haptic texture perception also reported consistent texture-selective activations in the parietal operculum and the insula. The latter activations comprised 3 of the 4 distinct cytoarchitectonic fields described on the human parietal operculum (Eickhoff, Amunts, et al. 2006; Eickhoff et al. 2007), namely the somatosensory OP1, OP4, and in particular OP3 (Stilla and Sathian 2008; Sathian et al. 2011). A recent study reported haptic texture-evoked activation in the collateral sulcus (CoS), close to a location showing activation in response to visual texture perception (Podrebarac et al. 2014). Similar texture-selective responses in the visual cortex, although located more posterior in the occipital cortex, were reported by Stilla and Sathian (2008) and Sathian et al. (2011) in response to both haptic and visual stimuli. Interestingly, 2 studies on the representation of material properties indicated that low-level image properties are represented in early visual cortex, whereas higher visual regions in the temporal cortex construct information about the perceptual visuo-tactile material properties (Hiramatsu et al. 2011; Goda et al. 2014).

Some studies specifically focused on roughness, and found that discrimination of this tactile texture dimension appears to systematically involve the parietal operculum when compared with macrospatial tasks such as length and shape discrimination (O'Sullivan et al. 1994; Ledberg et al. 1995; Roland et al. 1998). These results were confirmed by experiments focusing on variations in surface roughness: graded blood oxygen level-dependent (BOLD) effects were observed in the parietal operculum and the insula (Kitada et al. 2005; Simões-Franklin et al. 2011), but not in the S1.

Thus, taken together, the neuroimaging literature points to an involvement of the operculo-insular cortex in roughness estimation. Furthermore, based on the research on general texture processing (Sathian et al. 2011; Podrebarac et al. 2014) and perceptual material properties (Hiramatsu et al. 2011; Goda et al. 2014), an additional contribution of ventral temporal regions in roughness perception is possible. This contribution may have been missed by neuroimaging studies on roughness perception due to the limited sensitivity of the employed conventional univariate analysis methods. This part of the cortex was indicated in the processing of visual as well as non-visual perceptual material properties (e.g., smooth–rough) (Hiramatsu et al. 2011) and might be involved in haptic roughness perception via learned associations between visual and haptic texture properties as discussed by Podrebarac et al. (2014).

None of the haptic studies mentioned above allow inferences on the differential involvement of cortical regions in the processing of physical texture characteristics and their perceptual representation, as either multiple physical stimulus properties were varied at the same time or the mapping between physical and perceptual attributes was not taken into account. One particular stimulus set that allows us to dissociate the physical and perceptual stimulus space is a specially designed set of embossed dot patterns evoking different psychometric curves for 2 perceived texture dimensions, namely roughness and spatial density. This artificial stimulus set has been employed in several studies showing that perceived spatial density linearly decreases with increasing interdot spacing of the dot patterns (Merabet et al. 2004), whereas perceived roughness follows an inverted U-shape peaking at about 3 mm interdot distance (Connor et al. 1990; Merabet et al. 2004; Gescheider et al. 2005; Eck, Kaas, Mulders, et al. 2013; Gescheider and Wright 2013). Hence, perceived spatial density and perceived roughness of this stimulus set are both influenced by the number of texture elements, but only the former one can linearly be mapped to the physical stimulus space. This difference in complexity is also reflected at the afferent level, where the perception of spatial texture properties has been associated with the spatial code of slowly adapting type I cutaneous afferents (SA1; Johnson 2001), whereas roughness perception was influenced by a combination of different afferent channels. Taken together, these properties make this stimulus set ideal to investigate the cortical areas supporting the processing of the complex perceptual texture dimension roughness controlling for the processing of low-level sensory aspects by adding a spatial density judgment task.

Studies comparing the neural substrates of roughness and spatial density perception show inconclusive results. One of the few studies using the specific dot pattern stimulus set described above found that repetitive transcranial magnetic stimulation (rTMS) to the somatosensory cortex impaired roughness judgments, whereas judgments of spatial density were only altered after rTMS to the occipital cortex (Merabet et al. 2004). This could be interpreted as evidence that the percept of roughness is crucially dependent on somatosensory regions, whereas density and distance judgments mainly rely on the occipital cortex. However, this interpretation has found limited support up to now. As described above, roughness perception has been associated with the parietal operculum and insula (Kitada et al. 2005; Simões-Franklin et al. 2011). Moreover, an fMRI study using the same dot pattern stimuli and a similar design surprisingly found no regions with increased activations for a roughness estimation task, and indicated an involvement of early somatosensory and posterior parietal regions in tactile density estimation (Merabet et al. 2007). Also, a prior study by another group found that TMS targeting the somatosensory cortex had a disruptive effect on spacing discriminations as well (Zangaladze et al. 1999). Finally, our group found clear parametric effects of

stimulus spacing on the BOLD response in both early occipital and somatosensory regions (Eck, Kaas, Goebel, et al. 2013). Hence, there is evidence that, apart from the occipital cortex, density estimation might also involve the primary somatosensory areas. However, the contribution of each region is confounded by differences in the employed stimulus set and the task instructions [e.g., dot patterns and spacing estimation (Merabet et al. 2004) vs. linear gratings and discrimination (Zangaladze et al. 1999)].

Therefore, we set out to verify the differential contribution of the regions that were found to be involved in roughness and density estimation in a single fMRI experiment using the same stimuli for each task. We hypothesized that the cortical networks underlying density and roughness perception might specifically reflect the above-described differences in the complexity of both texture dimensions, that is, the mapping between the physical and perceptual space. To test this hypothesis, the current study used an integrative psychophysical and imaging approach, directly comparing a roughness estimation task with a spatial density estimation task of dot patterns varying in the mean center-to-center dot spacing, covering the full range of the psychometric curves. Our first aim was to characterize the cortical networks underlying density and roughness estimation, that is, haptic texture perception. Second, we aimed to investigate in which of these previously implicated brain regions, cortical activation varies with different levels of perceived texture characteristics, that is, perceived roughness and density. Since multivoxel pattern analysis (MVPA) is considered more sensitive than univariate data analysis methods to detect information in brain regions, we employed the former to reveal possible subtle differences in distributed activation patterns depending on the task context. Our third aim was to investigate to what extent similar effects can be observed for objective stimulus characteristics when subjects only focus on the stimulus exploration without a concurrent rating task. Hence, is enhanced attention to the stimulus characteristics a crucial factor, as indicated by Kitada et al. (2005)?

We expected spacing-related changes to be primarily reflected in early sensory regions, that is, the PoCG and the posterior occipital cortex, but roughness-related activation changes in higher-order cortical regions, that is, the insula and the parietal operculum, as observed in previous studies of roughness estimation by Zangaladze et al. (1999); Merabet et al. (2004); Kitada et al. (2005); Simões-Franklin et al. (2011) and possibly an involvement of regions in the ventral temporal cortex (VTC; Sathian et al. 2011; Podrebarac et al. 2014). We used an independent visual texture localizer run to identify regions in the temporal and occipital lobe possibly also involved in haptic texture processing, because the exact cortical locations of temporal and occipital cortical regions in haptic texture perception are still a matter of debate (Merabet et al. 2004, 2007; Sathian et al. 2011; Eck, Kaas, Goebel, et al. 2013; Podrebarac et al. 2014). To avoid bias, we also included areas in our analysis that were less consistently reported in the context of haptic texture perception, such as the posterior parietal cortex (PPC; Merabet et al. 2007) and the lateral prefrontal cortex (Kitada et al. 2005).

Material and Methods

Participants

Thirteen right-handed, healthy volunteers (9 women and 4 men) with normal or corrected-to-normal vision participated in the study. The mean age was 27 (range: 21–32) years. Subjects with calluses or (a history of) injuries to the hands were excluded from participation. All participants were graduate and undergraduate students at Maastricht University and received course credit or monetary compensation for their participation in the experiment. The local ethics committee approved the study and participants gave written informed consent. One subject (s04) had to be excluded from data analysis due to technical problems resulting in corrupted imaging data.

Stimuli

Visual Texture Localizer

The stimulus set consisted of 16 texture and 16 shape pictures as well as scrambled versions of the same images. Texture stimuli were grayscale top-view photographs of everyday textures, for example, abrasive paper, cork, carpet, foam material, wallpaper, Nepal wool, and felt. All texture stimuli were the same size. Shape stimuli were grayscale images of abstract 3D shapes, all made of the same material and with approximately the same size. The shape photographs were taken from a slightly tilted front-view perspective to emphasize the three-dimensional characteristic of the objects. Since the images varied slightly in size, a gray circle area with a radius of 200 pixels was created around each picture to match the size of the stimulated visual field across both categories. Scrambled versions of all stimuli were generated by segmenting the image (including the gray circle area) into 64 pixel blocks and rearranging them by generating random permutations of the blocks in the image. In order to control for differences in low-level visual properties between image categories, the luminance and contrast of each image were adjusted to match the average luminance and contrast of the stimulus set. The background of all pictures was set to black (Fig. 1). No analysis was based on the scrambled images in the present study, but these stimuli were included for another functional localizer experiment.

Haptic Texture Exploration Tasks

Haptic stimuli consisted of six 5×5 cm^2 plastic dot pattern textures. Each dot was 0.8 mm in diameter and 0.6 mm in elevation. The dots were arranged non-periodically on the plates. The only characteristic that varied between the textures was the mean center-to-center dot spacing and hence the number of texture elements (Fig. 2). Details about the algorithm used to produce these textures can be found in Eck, Kaas, Mulders, et al. (2013). It has been found that haptic roughness perception of these dot pattern textures follows approximately an inverted U-shape curve, peaking at about 3–4 mm interelement spacing (Connor et al. 1990; Merabet et al. 2004, 2007; Gescheider et al. 2005; Eck, Kaas, Mulders, et al. 2013). On the other hand, for density and distance perception, a linear function can be expected with increasing interdot spacing (Merabet et al. 2004; Eck, Kaas, Goebel 2013). Using the same stimulus set to sample the roughness and density curve at different curve sections allows us to identify cortical responses that vary with perceived stimulus characteristics, rather than purely presenting differences in the physical stimulus properties (i.e., interelement spacing). The interdot spacing of the textures selected for this study was 1.50, 2.25, 3.50, 4.50, 5.50 and 8.25 mm. Figure 3 illustrates the locations of these textures on the perceived roughness and density curve [as hypothesized based on previous behavioral studies (Merabet et al. 2004; Eck, Kaas, Mulders, et al. 2013)].

Experimental Set-up

We used a similar experimental set-up as published previously (Eck, Kaas, Goebel 2013). All dot pattern stimuli were placed on

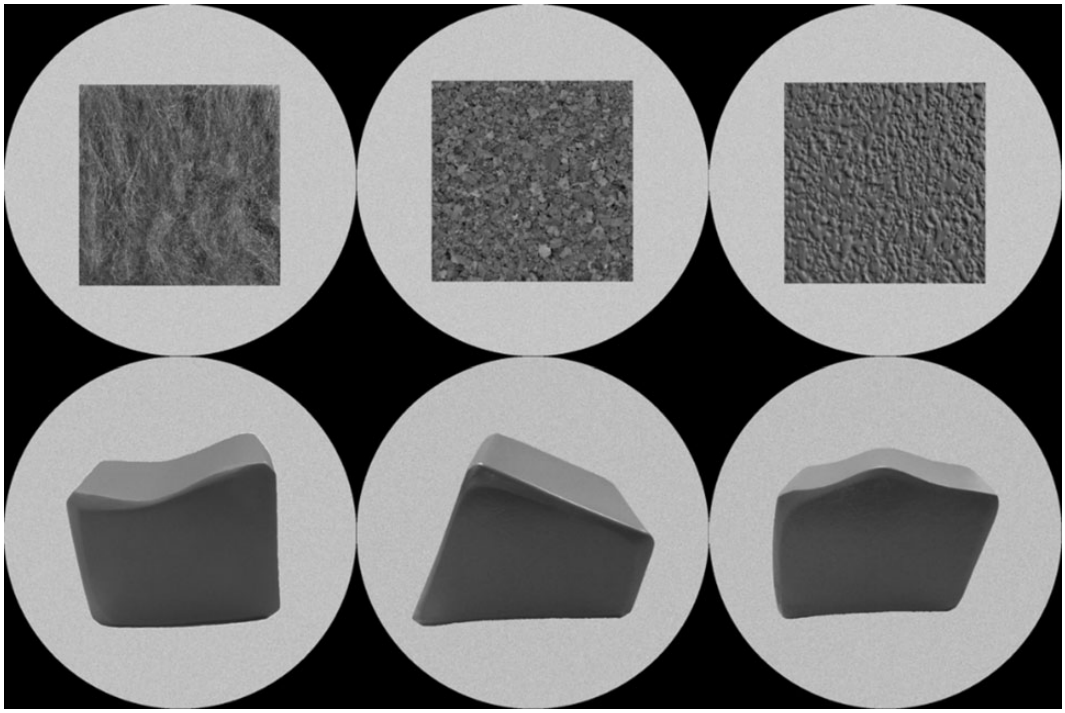

Figure 1. Examples of stimuli used in the visual texture localizer runs. Top row: textures. Bottom row: shapes.

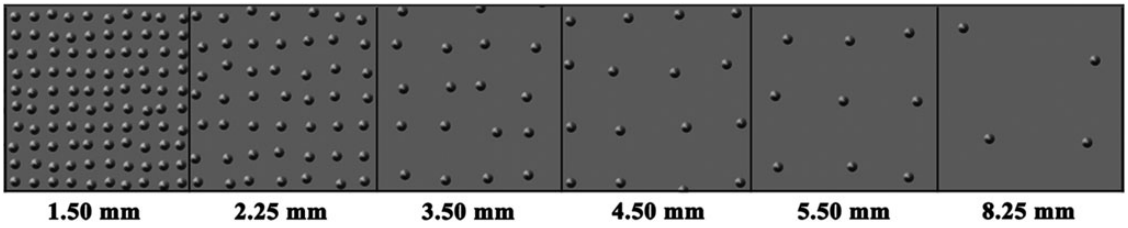

Figure 2. Magnified excerpts of the dot pattern textures used in the haptic experimental runs.

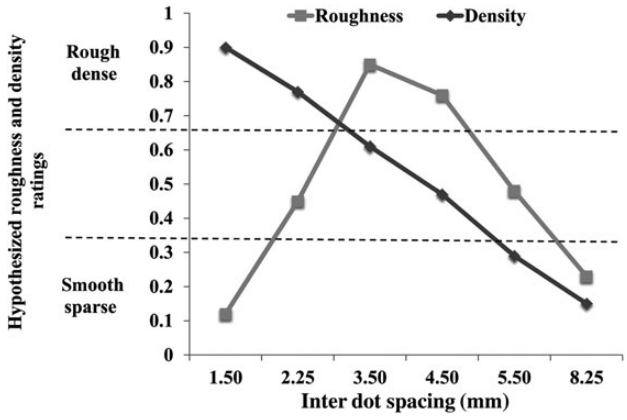

Figure 3. Schematic representation of the stimulus space with regard to the expected roughness and density ratings.

a circular wooden board, covered by another plate with a rectangular cutout that ensured that subjects could touch only a single texture. The entire presentation device was placed over the thighs of the participant and was attached to the scanner table. The right hand of the subject, meant to explore the textures, was placed on top of the cover plate, whereas the left hand, that operated the button box, lay next to the participant's legs. To reduce movement during the scanning, both arms were supported by foam padding. The experimenter, who was standing next to the scanner bore, controlled the presentation of the haptic stimuli. Visual cues were displayed centrally on a black background. The images were projected onto a rear-projection screen at the end of the scanner bore and subjects viewed the stimuli via a mirror mounted to the head coil. Stimulus timing and presentation was controlled by the Presentation® software (Neurobehavioral Systems, Inc., Albany, CA, USA).

Experimental Procedure

Visual Texture Localizer

Texture and shape images as well as scrambled versions of both categories were presented in separate blocks of 8, each block lasting 16 s. The 4 different block types (i.e., texture, shape, scrambled texture, and scrambled shape) were interleaved with 16 s blocks of rest. Each image was presented 3 times during the independent localizer run.

Both stimulus presentation within category blocks and the order of blocks was randomized. For task blocks, subjects were informed about the category of the next block (i.e., "Scrambled",

"Texture", or "Shape") by an auditory cue via headphones 700 ms before block onset. The beginning of the rest interval was cued by the word "Rest". After the last image in each texture and shape block, a question was displayed asking whether the last item presented was presented before in the same block. This task was chosen to ensure subjects' attention to the images. Subjects responded by pressing 1 of 2 buttons on a response box attached to their left hand. For the scrambled texture and shape blocks, subjects were instructed to passively view the images. During picture presentation, a red fixation dot was displayed in the center of the screen, whereas a white fixation dot was presented during rest blocks. Participants were asked to fixate on these dots during the localizer run.

Haptic Texture Exploration Tasks

Subjects were informed that they would be presented with one haptic texture at each trial. In "Rating" runs, participants had to judge the perceived roughness or spatial density after stimulus presentation, whereas in the "No-Estimation" runs subjects were told to focus on the haptic exploration of the textures. The experimenter stressed the importance of focusing on the mere stimulus exploration in the No-Estimation runs as in contrast to judging the perceived stimulus properties in the Rating runs. Participants explored the textures by sweeping 4 times with their right index-, middle-, and ring fingers (simultaneously) across the surface. After this exploration movement, subjects placed their hand back in the resting position on top of the wooden cover plate. In the Rating runs, the haptic exploration interval (4 s) was followed by a jittered delay (5–9 s) and a rating time window (3 s). These task trials alternated with rest intervals of 12–14 s (jittered). During the rating time window, subjects were asked to judge the perceived roughness or density of the previously explored dot pattern on a 400 pixel visual analog scale (VAS) ranging from very smooth/sparse to very rough/dense. The slider of the VAS was moved to the left or to the right by pressing 2 buttons on a fiber-response box attached to the subject's left hand. In the beginning of the rating interval, the slider was positioned in the middle of the scale. In the No-Estimation runs, exploration was immediately followed by a rest time window (Fig. 4). Auditory cues delivered via headphones in the intertrial intervals (rest) instructed the experimenter to turn the haptic presentation device to the correct stimulus for the next trial. Subjects in turn used visual cues to identify the correct trial phase. A red dot presented in the center of the screen indicated the haptic exploration interval, a blue dot marked the delay period, and a white dot presented the rest interval. Density and roughness conditions were blocked in the Rating runs and the words "Roughness" and "Density", displayed on the screen in the beginning and the middle of the runs, indicated the task for the upcoming trials. The labeling of the endpoints of the VAS was adapted to the task condition. The order of the task blocks was varied across runs and was changed for all participants. Each of the 6 dot patterns was repeated 15 times in each task condition (roughness vs. density rating vs. no-estimation) over the course of the fMRI experiment.

Each subject participated in 3 experimental sessions on 3 different days. In the first experimental session, subjects were familiarized with the Rating and No-Estimation runs in a mock scanner. This was done to minimize movement artifacts in the following scanning sessions. Subjects practiced the exploration movement, and were introduced to the VAS and the sensitivity of the response button box. Participants were instructed and trained to perform an exact onset and offset of the exploration movement in synchrony with the color changes in the fixation dot. Furthermore, they were asked to use the same movement timing, movement direction, and contact force for all trials. The same stimuli as in the fMRI experiment were used in the practice session to familiarize participants with the stimulus range; each stimulus was repeated 4 times within the 3 task conditions. The practice session lasted until: (1) Subjects were comfortable with the tasks, (2) the movement was experienced by the subject as effortless, (3) the movement was synchronized with the duration of the exploration interval, and (4) all other motion was reduced to a minimum. The average duration of the mock scanner session was approximately 30 min. The second session consisted of the visual texture localizer run and 5 No-Estimation runs, each 170 volumes long and therefore lasting about 6 min. In the third session, participants completed the 5 Rating runs, each 510 volumes long, lasting 17 min. Data for the Rating and No-Estimation runs were acquired in different sessions to keep the scanning time in each session within a reasonable timeframe.

Data Acquisition

Data were acquired at the Maastricht Brain Imaging Center (Maastricht, The Netherlands) with a 3-T Siemens Allegra MR head scanner equipped with a standard quadrature birdcage coil. In both scanning sessions, a standard anatomical T_1-weighted data set was acquired using a magnetization-prepared rapid acquisition gradient-echo (MPRAGE) sequence covering the whole brain [repetition time (TR) = 2250 ms, echo time (TE) = 2.6 ms, flip angle (FA) = 9°, matrix: 256 × 256, voxel size: 1 × 1 × 1 mm, 192 slices]. In the first scanning session, this was followed by the 5 No-Estimation runs, a short break, and the visual texture localizer run, whereas in the second scanning session the anatomical image acquisition was followed by the 5 Rating runs. All functional images were obtained with a T_2^*-weighted echo-planar imaging sequence (TR = 2000 ms, TE = 30 ms, FA = 90°, matrix: 64 × 64, field of view: 224 × 224, slice thickness = 3.5 mm, 32 slices covering the whole brain, no gap).

Data Analysis

Trials in which subjects either missed the exploration or the rating interval of the haptic stimulus, or for which the timing of the exploration movement was incorrect, were removed from behavioral and fMRI data analysis. One subject missed 4 of 90 trials in the density rating task; in all other subjects, the number of missed/incorrect trials did not exceed two for any of the task conditions.

Behavioral Data Analysis

To evaluate the variability of the ratings across subjects and repetitions, the mean roughness and density curve was assessed for each subject (Fig. 5). For the majority of subjects, the mean roughness and density curve was comparable with the results of our previous behavioral study (Eck, Kaas, Mulders, et al. 2013). However, for some of the participants perceived roughness did not decrease as much for wider interdot spacing as was hypothesized based on the literature using similar stimuli (Connor et al. 1990; Merabet et al. 2004, 2007; Gescheider et al. 2005; Gescheider and Wright 2013). This high interindividual variability was not expected, but the minimally sampled stimulus space with 6 stimuli only versus 29 stimuli in our earlier study might have influenced the results. Subjects who did not show a decrease in perceived roughness below the middle of the VAS scale (0) for wide dot spacing textures had to be excluded from data analysis, because an unambiguous categorization of stimulus spacings to different

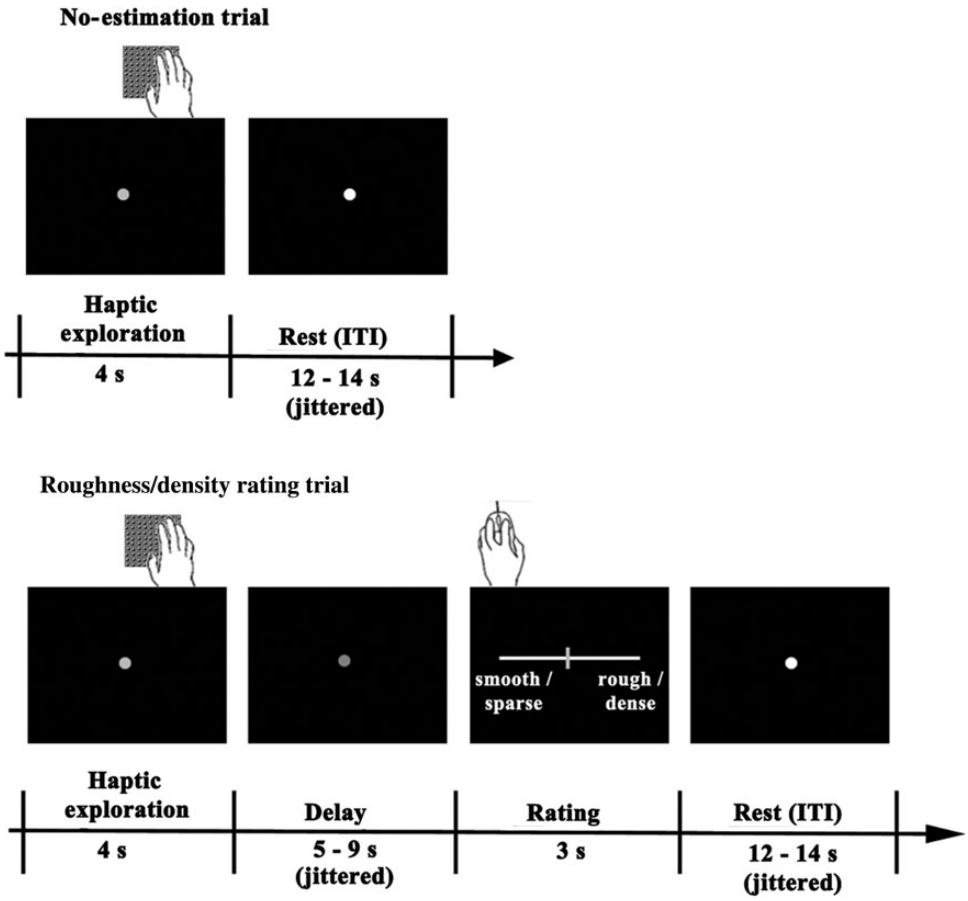

Figure 4. Illustration of the experimental trials for the No-Estimation and Rating runs. ITI: intertrial interval.

roughness classes (independent from perceived density) was not possible. This was important as a combination of a rating and spacing criterion was used to assign stimuli to the low roughness category in order to avoid a complete overlap with the high density category for the multivariate analysis of the fMRI data (see details below). To ensure that trial labels could be defined unequivocally, we avoided an overlap in behavioral ratings between trials of different categories of the same perceived texture characteristic. Therefore, participant s05, s06, s09, and s13 were excluded from the data analysis and are not considered in the following descriptions.

For multivoxel pattern classification, we grouped the fMRI trial data into categories. Based on the mean roughness and density ratings, trial categorization to low and high density/roughness classes was performed as follows. For the high density and roughness class, we selected the 2 dot pattern textures with the highest mean ratings. Hence, for all subjects, the trials with 1.50 and 2.25 mm interdot spacing were categorized as high density, whereas the 3.50- and 4.50-mm stimuli were grouped to a high roughness class. For the low density class, we selected the 2 stimuli with the lowest mean density ratings over all repetitions, that is, 5.50 and 8.25 mm interdot spacing for all subjects. For the low roughness class, we combined this rating criterion with a spacing criterion. We selected the stimulus with the lowest roughness rating in the wide interdot spacing range (4.50–8.25 mm), that is, 8.25 mm for all subjects, and the stimulus with the next lowest roughness rating in the close interdot spacing range (1.50–3.50 mm), that is, 1.50 mm for 5 of 8 subjects and 2.25 mm for 3 of 8 subjects. This ensures that an above-chance classification of the high and low roughness category is neither confounded with stimulus spacing nor with perceived density.

To ensure unambiguous category representations, individual trials with ratings that could not be clearly assigned to either the high or low category (border trials) were excluded from data analysis. Trials in the No-Estimation runs with the same interdot spacing stimuli as in the high and low density categories of the Rating runs were grouped in a close and a wide spacing category. An overview of trial categorization can be found in Table 1. Task classification, that is, trials in the roughness task blocks versus density task blocks, was based on all dot pattern textures. The rationale of this analysis was to investigate the effect of task instructions independently of the objective stimulus space.

fMRI Data Preprocessing

Functional and anatomical data were analyzed with BrainVoyager QX 2.4.2 (Brain Innovation, Maastricht, The Netherlands). The first 2 scans of each functional run were discarded to allow for T_1 equilibration. Preprocessing of the functional data included: slice scan time correction, intrasession alignment to detect and correct for small head movements by rigid body transformations, temporal filtering removing linear trends, and nonlinear temporal frequencies of 3 or less cycles per run. No subjects had to be removed because of excessive head motion. Functional images of all runs were coregistered to the anatomical volumes of the respective subject and scanning session and

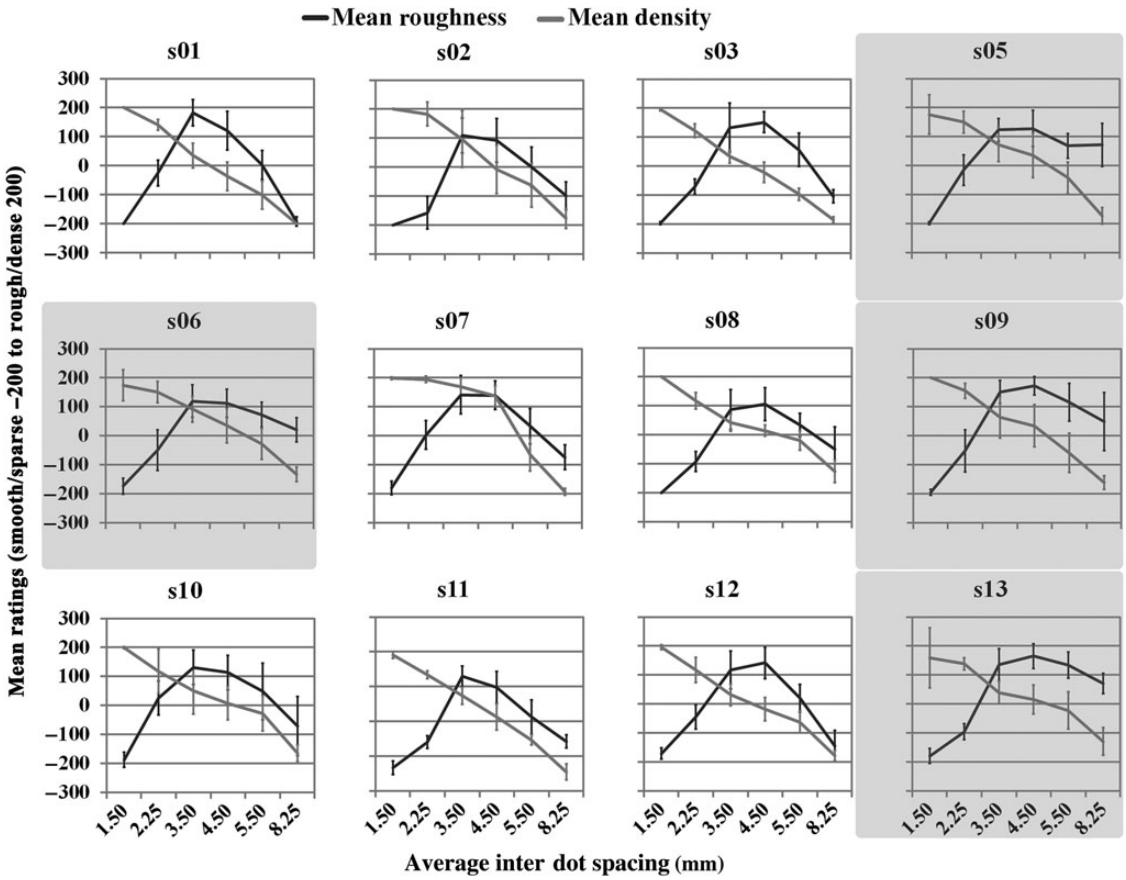

Figure 5. Mean density and roughness ratings for all dot pattern textures averaged over all repetitions and separately for all subjects. Error bars represent the standard deviation. Subjects highlighted in gray were excluded from all subsequent analyses.

Table 1 Summary of trial categorizations to roughness (R), density (D), spacing (S), and task classes

Subject	Dot pattern spacings grouped in high/high/close category			Dot pattern spacings grouped in low/low/wide category			Number of trials in categories (high/high/close/R-task, low/low/wide/D-task)			
	R	D	S	R	D	S	R	D	S	Task
s01	3.50	1.50	1.50	1.50	5.50	5.50	29[a]	30	30[a]	R: 89[a]
	4.50	2.25	2.25	8.25	8.25	8.25	30	29[a]	30	D: 89
s02	3.50	1.50	1.50	2.25	5.50	5.50	27[a]	29	29[a]	R: 84[a]
	4.50	2.25	2.25	8.25	8.25	8.25	28	28[a]	30	D: 86
s03	3.50	1.50	1.50	1.50	5.50	5.50	29[a]	30[a]	30[a]	R: 88[a]
	4.50	2.25	2.25	8.25	8.25	8.25	29	30	30	D: 90
s07	3.50	1.50	1.50	1.50	5.50	5.50	28[a]	29	29[a]	R: 86[a]
	4.50	2.25	2.25	8.25	8.25	8.25	28	28[a]	30	D: 87
s08	3.50	1.50	1.50	2.25	5.50	5.50	27[a]	28[a]	30[a]	R: 84[a]
	4.50	2.25	2.25	8.25	8.25	8.25	27	28	30	D: 86
s10	3.50	1.50	1.50	1.50	5.50	5.50	27	28	29[a]	R: 83[a]
	4.50	2.25	2.25	8.25	8.25	8.25	26[a]	27[a]	30	D: 85
s11	3.50	1.50	1.50	2.25	5.50	5.50	27[a]	30[a]	30[a]	R: 85[a]
	4.50	2.25	2.25	8.25	8.25	8.25	28	30	30	D: 90
s12	3.50	1.50	1.50	1.50	5.50	5.50	29[a]	30	30[a]	R: 87[a]
	4.50	2.25	2.25	8.25	8.25	8.25	29	29[a]	30	D: 89

Note: All dot pattern spacings were used in the Roughness–Density Task Classification.
[a]Number of trials per class used for both categories in the MVPA.

transformed into Talairach space resulting in an interpolated functional voxel size of 3 × 3 × 3 mm. Based on the T_1-weighted anatomical data sets, individual surface reconstructions of the cortical sheet were created employing an automatic white–gray matter segmentation approach. Segmentation errors of the automatic procedure were manually post-corrected. These individual cortical surfaces were aligned to a moving target group average by using a curvature-driven cortical mapping approach (Goebel

et al. 2006; Frost and Goebel 2012). The results were used to create an average cortex representation of all subjects. Furthermore, the mapping parameters from cortex-based alignment (CBA) were used to align individual statistical maps to the group-average cortical surface.

Univariate Data Analysis

For group analysis, a whole-brain fixed-effects regression analysis (FFX) was chosen because of the sample size of $N = 8$ [after removal of participants with corrupted data (s04) and similar roughness and density rating curves (s05, s06, s09, and s13)]. Three different general linear models (GLMs) were used to address different aspects of the research question.

The first model was comprised of 7 predictors. All spacing trials of the roughness task condition were grouped to one predictor and the same was done for all trials in the density task blocks. These 2 predictors were defined for each of the 3 trial intervals, that is, haptic exploration, delay, and rating interval. The presentation of the visual cues "Roughness" and "Density" during the experimental runs was modeled as the seventh predictor. One contrast was computed for that model asking for differences between the roughness and density task during haptic exploration, irrespective of the stimulus characteristics ("Exploration: roughness ≠ density").

In a second model, task-related predictors were defined based on the trial categorization in the Rating runs as explained above. There were 3 rating categories: high, low, and a residual category for trials that could not be assigned to the high or low category. This resulted in a total of 19 predictors (3 trial phases [exploration, delay, rating] × 2 haptic tasks [roughness, density] × 3 categories [low, high, remaining trials] + 1 visual cue predictor). Two different contrasts were computed for the haptic exploration interval of that model, namely "Exploration: high roughness ≠ low roughness" and "Exploration: high density ≠ low density".

The third model is based on the No-Estimation runs. Three predictors were defined, representing trial categorization with regard to the objective stimulus characteristics, that is, interdot spacing of the textures. Two predictors contained the close and wide interdot spacing trials, whereas a third predictor represented the remaining dot pattern trials. The contrast computed for that model compared close and wide spacing trials ("Exploration: close spacing ≠ wide spacing").

All predictor time courses were convolved with a two-gamma hemodynamic response function to account for the hemodynamic response delay. The voxel threshold for statistical significance was first set to $\alpha = 0.005$ uncorrected, and all statistical contrast maps were then corrected for multiple comparisons using cluster size thresholding (Forman et al. 1995; Goebel et al. 2006) with a cluster-level false-positive rate of $\alpha = 0.05$.

Multivariate Data Analysis

To reduce the number of initial features for multivariate data analysis, anatomical and functional masks were defined on the individual cortical meshes.

Anatomical Cortex Masks. Anatomical regions of interests (ROIs) were delineated on the individual cortex meshes. All regions, including the S1, were defined bilaterally, because recent studies also show a contribution of the ipsilateral S1 in tactile stimulus anticipation (van Ede et al. 2014) and learning (Sathian et al. 2013).

The PPC region included the superior parietal and inferior parietal lobule—separated by the intraparietal sulcus (Culham and Valyear 2006). The second region, which included the S1, was defined by the location of the PoCG and the central sulcus (CS; Sanchez-Panchuelo et al. 2010; Stringer et al. 2011).

The third region, operculo-insular cortex (OpIns cortex), circumscribed the insular cortex and the parietal operculum on which the human secondary somatosensory cortex (S2) is located (Eickhoff et al. 2007, 2008; Mazzola et al. 2012). The fourth anatomical ROI was the frontal/prefrontal cortex. The approximate boundaries of this cortical patch were defined as follows. The posterior boundary was the inferior precentral sulcus (PreCS) and the superior boundary was the superior frontal gyrus. The inferior boundary was the inferior frontal gyrus and the anterior boundary was up to, and including, the lateral part of the frontopolar prefrontal cortex. The coverage of the anatomical masks was intentionally slightly bigger than in conventional studies (e.g., Goulas et al. 2012) to account for interindividual differences in anatomical–functional correspondence.

Functional Cortex Masks. Based on the functional localizer run, a regression analysis was computed with 6 predictors: Texture block, Shape block, Scrambled texture block, Scrambled shape block, Question, and Response. To identify regions in the temporal and occipital lobe that show a tendency to respond stronger to texture than to shape images within our sample of $N = 8$, we ran the above-described GLM first at the FFX level, with a temporal and occipital lobe mask for all participants, comparing texture and shape blocks (Texture block > Shape block). We identified a bilateral posterior occipital cortex cluster (pOCC) and a bilateral cluster in the VTC bordering the fusiform gyrus (FG) and the CoS (Fig. 6A). Afterwards, we ran the same model and contrast on the single-subject level, identifying activation clusters in each individual subject. Statistical maps were thresholded as described above. The number of voxels in the resulting clusters varied substantially between individuals. To reduce size differences between the anatomical and functional cortex masks, we defined the 4 subject-specific cortex masks in the temporal and occipital lobe as 800 voxel regions around the cluster-specific peak voxels in the individual Texture versus Shape contrast. Significant activation clusters were identified in 7 of 8 subjects in the left hemisphere of the posterior occipital cortex; this was also true for 6 of 8 participants in the right pOCC and the left VTC. Above-threshold activations were, however, only present in 3 of 8 subjects in the right VTC. For participants in which any of the 4 regions were not present in the thresholded individual contrast maps, the subject-specific peak voxel within the respective FFX cluster was determined and used as the origin of the mask definition. A summary of the subject-specific peak voxels can be found in Table 2.

The location of the bilateral masks is illustrated on the right average cortex representation in Figure 6B. Due to interindividual differences in anatomy, no perfect overlap of individual cortex masks and the subject-averaged folding pattern of the cortical sheet can be expected even after macroanatomical alignment (CBA).

Four different models were considered for multivariate pattern analysis on single-subject level, separately for all 6 individual cortex masks: (1) roughness versus density haptic exploration trials (Rating runs), (2) high versus low density haptic exploration trials (Rating runs), (3) high versus low roughness haptic exploration trials (Rating runs), and (4) close versus wide spacing haptic exploration trials (No-Estimation runs). Mask voxels with a mean

raw signal intensity below 70 and a standard deviation below 1 were excluded from data analysis to reduce noise in the data. Single-trial estimation was performed by creating separate multivoxel response patterns for all trials, subjects, region masks, and models. The response pattern of a single trial was estimated by extracting the average signal for TR 2, 3, and 4 after onset of the haptic exploration interval. This signal was transformed to percent signal change by dividing it by the mean baseline signal of

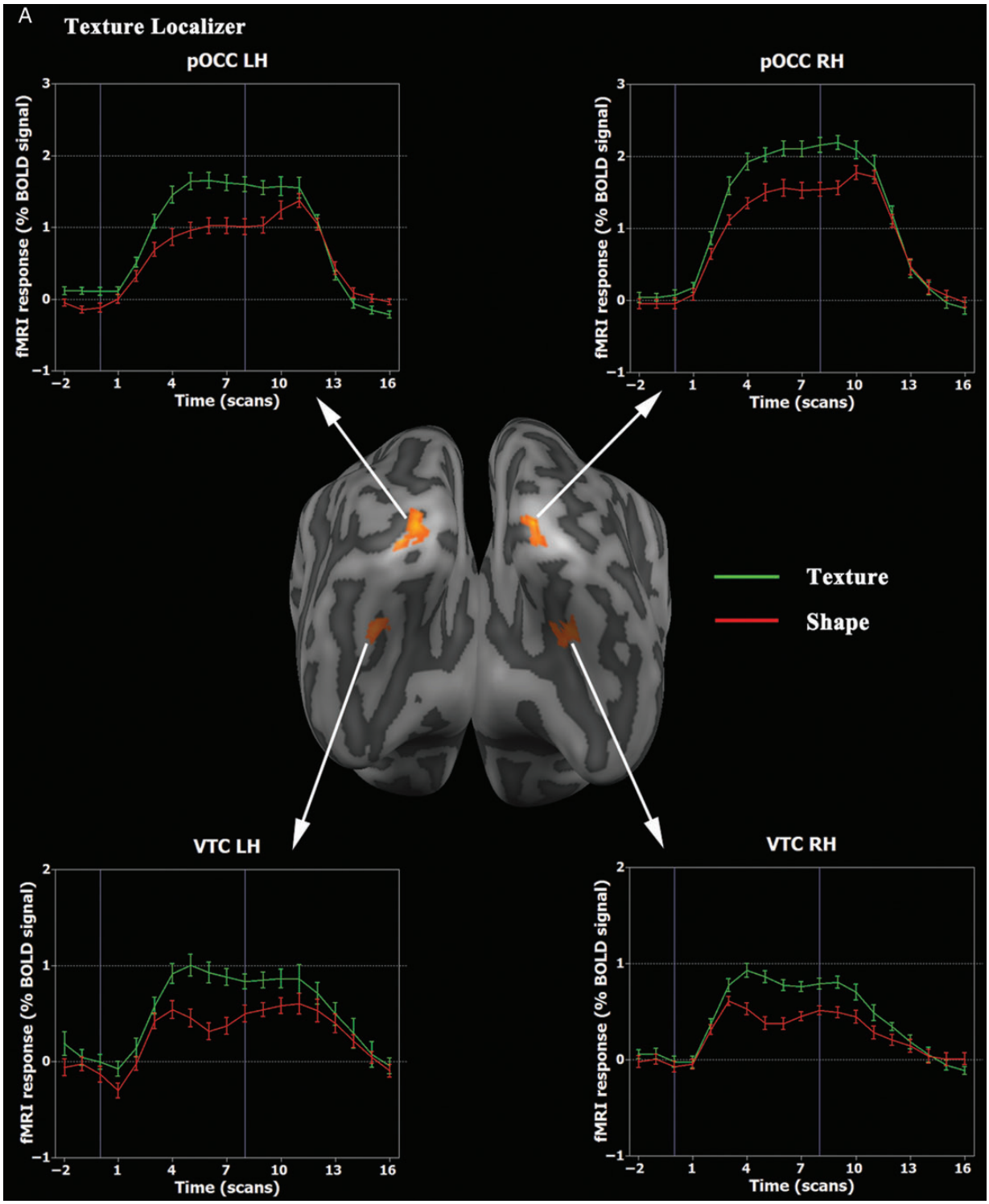

Figure 6. Anatomical and functional masks. (*A*) FFX contrast map of the texture localizer: Texture block > Shape block overlaid on the average cortex reconstruction of all subjects. (*B*) Probability map of individually defined cortex masks illustrated on the average cortical sheet of the right hemisphere. Only vertices that are represented in 6 of 8 subjects' masks are color-coded. PPC: posterior parietal cortex; PoCG: postcentral gyrus; CS: central sulcus; PFC: prefrontal cortex; pOCC: posterior occipital cortex; VTC: ventral temporal cortex.

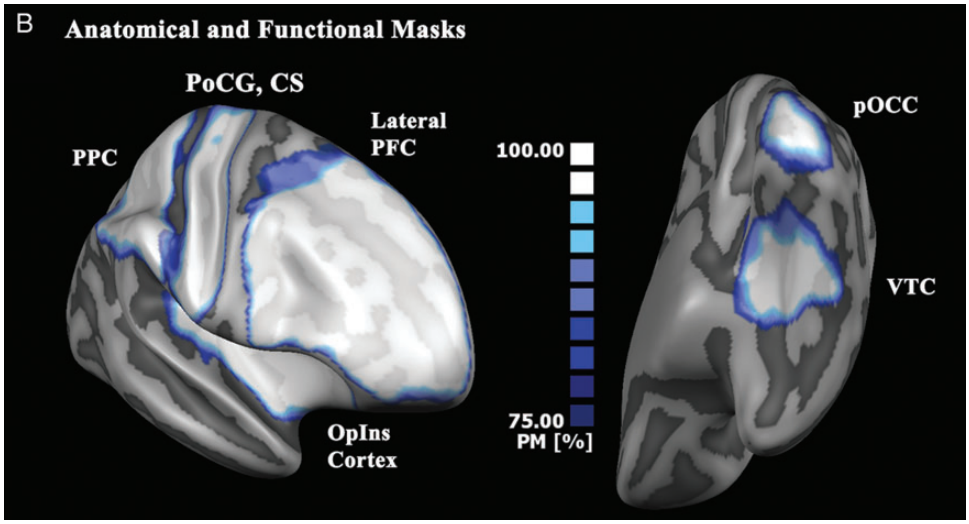

Figure 6. Continued

Table 2 Individual peak voxels in the occipital and temporal lobes of the contrast maps: Texture block > Shape block

Subject	Right pOCC		Left pOCC		Right VTC		Left VTC	
	Talairach coordinate		Talairach coordinate		Talairach coordinate		Talairach coordinate	
	x, y, z	t-value	x, y, z	t-value	x, y, z	t-value	x, y, z	t-value
s01	17, −98, 0	5.8	−25, −92, −6	8.2	26, −44, −15	5.6	−34, −47, −15	6.2
s02	20, −101, 0	7.5	−13, −92, 0	10.2	29, −56, −9	4.3[a]	−25, −59, −12	6.8
s03	8, −92, −18	3.9	−19, −95, −21	4.6	23, −41, −18	3.6[a]	−28, −53, −18	2.6[a]
s07	14, −83, −6	6.9	−25, −92, −9	6.8	20, −50, −12	5.8	−28, −59, −18	5.7
s08	17, −95, −6	5.7	−16, −92, −3	7.1	24, −53, −15	3[a]	−19, −59, −24	5.9
s10	11, −95, −6	3.6[a]	−16, −92, −15	5.8	23, −38, −15	4.3[a]	−25, −35, −18	5.5
s11	14, −92, −6	3.2[a]	−25, −89, −3	3.6[a]	32, −56, −9	3.1[a]	−25, −56, −15	2.4[a]
s12	8, −92, −21	4.7	−13, −101, 6	5.4	29, −26, −18	5.3	−28, −65, −15	4.8

Note: Talairach coordinates of the peak voxels with the respective t-values.
[a]Individual peak voxels in FFX clusters.

TR −2, −1, 0 with regard to stimulus onset and multiplying it by 100. The extracted single-trial responses of each voxel were normalized by subtracting the mean and dividing by the standard deviation of the training trials of the respective voxel. Depending on the trial categorization scheme of the 4 different models, trial response patterns were labeled according to the classes described above (low/high density/roughness/spacing or density vs. roughness trials irrespective of the stimulus differences). See Table 1 for the number of trials per class and subject. To equalize the number of trials per class in each model, we used as many trials for analysis as were available in the class with the lowest number of trials (marked in the footnote "a" of Table 1). These trials were selected randomly. However, within a subject and model, the same number of trials was used for both classes.

For analysis of the multivoxel patterns, we combined linear support vector machines (SVMs) with an iterative multivariate voxel selection approach—recursive feature elimination (RFE; De Martino et al. 2008)—in order to remove non-informative voxels that can degrade classification performance. For classifier training, we used a training set containing 20 of all category trials for the roughness, density, and spacing model and 60 trials for the task model. The test set used for assessing the performance and generalization ability of the classifier consisted of the remaining trials. The RFE algorithm started with the full number of voxels in the masks. At each RFE iteration, 2/3 of the training data were used to train a least square SVM (ls-SVM; Suykens et al. 2002). The classification model (i.e., weights) was used to create discriminative maps that indicate the importance of each voxel to class discrimination. There were 20 iterations, each repeating this procedure with a different subset of training trials. Each RFE voxel selection level was concluded by averaging the discriminative weights for each voxel over the 20 iterations, ranking the average discriminative weights and discarding voxels among the lowest 6% corresponding to the smallest ranking. The number of RFE voxel selection levels was adapted to the initial mask size and ranged from 61 to 84.

The entire RFE procedure was performed in 20-fold cross-validation. See Figure 7 for a summary of the multivariate analysis approach. The final accuracy at each RFE voxel selection level was computed as the mean over these 20 cross-validations. The classification performance reported below represents the average maximum accuracy across all RFE voxel selection levels.

A two-step procedure was used to assess whether the difference between the actual accuracy and the empirical chance level was significantly above 0 across subjects for a specific model and region. In a first step, permutation tests were performed for each

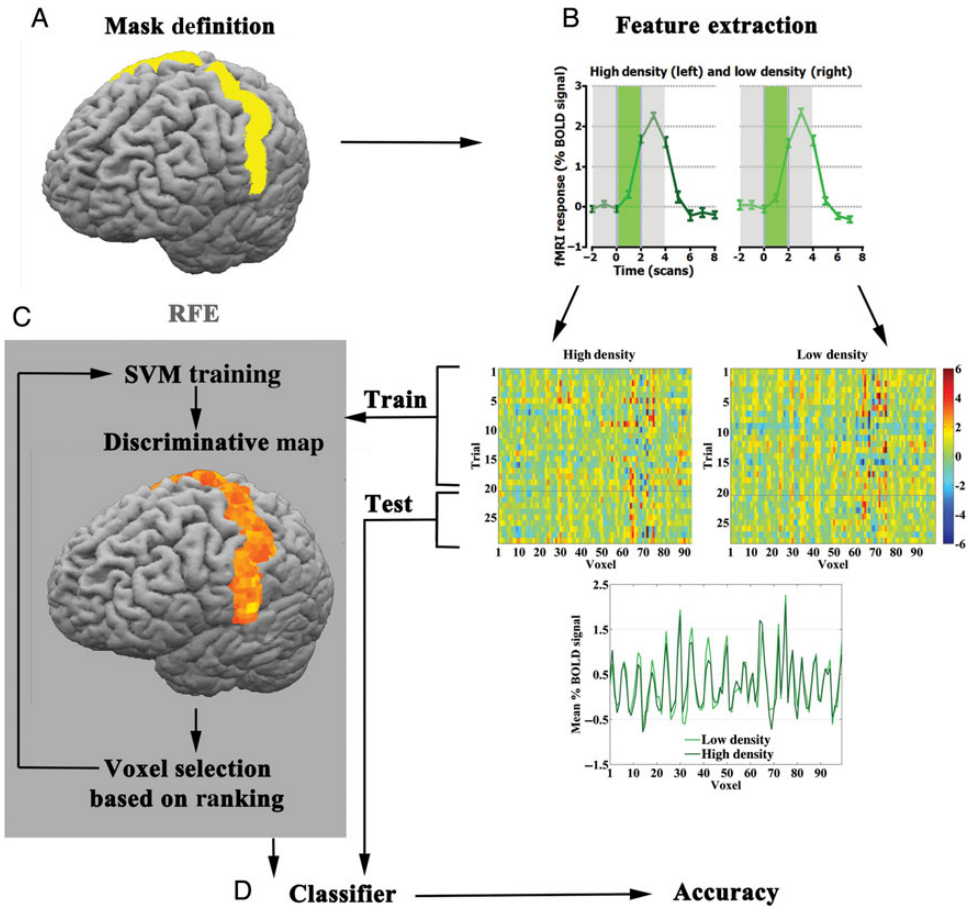

Figure 7. Overview of the multivariate data analysis illustrated on the high/low density classification within the PoCG mask of a single subject. (*A*) fMRI time course data were extracted from all voxels within the defined mask. (*B*) Features were defined for all trials and for each density class separately by selecting the mean signal of the second, third, and fourth scans after stimulus onset, visualized by the second gray segment in the upper row plots. This stimulus-related signal was percent-normalized using the baseline signal, represented by the first gray segment in the same plots. The green demarcated time interval represents the stimulus duration of 4000 ms. The lower two plots show the multivoxel response patterns of all trials within both categories for 100 out of the initial 1800 PoCG mask voxels of that participant. The plot below represents the averaged pattern over all trials for the same 100 voxels, separately for both density classes. (*C*) The RFE approach was used to reduce the number of voxels and select the pattern with the most discriminative information. (*D*) An independent set of test trials was used to test the generalization performance of the classifier.

subject and ROI. We used exactly the same feature extraction and SVM–RFE combination approach as explained above, but labels were randomly assigned to trial response patterns and the permutation was repeated 100 times. The final accuracy value of a single permutation was defined as the maximum prediction accuracy across all RFE steps, averaged over all cross-validations. The accuracies of all 100 permutations represent the permutation distribution of the chance level. The medians of these subject-specific null-distributions were used in the second step employing an exact permutation test. Assuming that the null hypothesis is true, namely that the actual accuracies across subjects are at chance level, multiplying any of the subjects' difference (actual accuracy – median permutation accuracy) by −1 will have no effect on the correctness of the null hypothesis. Considering a sample size of 8 subjects, there are 2^8 (256) permutations possible. These permutations constitute an estimate of the statistical distribution of the random effects (RFX) null hypothesis. Above-chance classification across subjects was assumed when the mean of the subject-specific differences was at or above the 95th percentile of the null distribution.

To visualize regions that are involved in task or roughness/density/spacing classification across subjects, single-subject maps were combined to a discriminative group map. For each subject, a map was created showing voxels that survived at least 25% of the RFE voxel selection levels. These maps were sampled on the reconstructed cortex of each subject and aligned to the group-average cortex mesh using the CBA parameters. To combine the single-subject maps to a group map, only vertices that were present in at least 6 of the 8 single-subject maps were color-coded. The group-average map was thresholded by applying a cluster size threshold of 25 mm^2. This approach was applied for each model and region mask.

Results

Univariate Data Analysis

A direct statistical comparison of the haptic exploration interval in the density and roughness estimation task, irrespective of the stimulus spacing, showed no significant difference in the univariate activation maps for both tasks. The same was true for the comparison between low and high roughness trials in the roughness rating task and wide and close spacing trials in the No-Estimation runs. Only the comparison of high versus low

density trials in the density rating task revealed significantly lower activations for high density trials (close stimulus spacing) in the ipsilateral PoCG extending into the postcentral sulcus (PoCS; peak voxel: $t_{(20184)} = -4.43$, $P < 0.001$), including Brodmann's area 1 (BA1). An event-related average showed that this effect represents differences above baseline level (Fig. 8).

Multivariate Data Analysis

Effects of Task Instructions

For the task classification, haptic exploration trials were labeled according to the task instructions, that is, roughness versus spatial density estimation, irrespective of the perceived texture properties. The classifier performance of distinguishing fMRI patterns elicited by haptic texture exploration between the 2 tasks was significant at the group level for both early sensory and higher-order brain regions. The mean accuracy across all 8 subjects reached 56.5% in the PoCG (chance level: 51.6%, $P = 0.004$). This was significantly above the empirical chance level as determined by the exact permutation test. Similar results were obtained in all other ROIs. Both the mean classification accuracy of 57.9% (chance level: 51.3%, $P = 0.004$) in the operculo-insular region and of 58.7% (chance level: 51.5%, $P = 0.004$) in the PPC were significant at the group level. Significant above-chance classification was also confirmed for the lateral prefrontal cortex (58.9%, chance level: 51.7%, $P = 0.008$), the posterior occipital cortex (56.1%, chance level: 51.6%, $P = 0.012$), and the VTC (56.2%, chance level: 51.4%, $P = 0.024$). As all regions showed significant above-chance classification, we tested the validity of the chosen approach by performing the task classification in a control region, that is, the Heschl's gyrus. In this region, the classifier performance did not exceed the empirical chance level (52.4%, chance level: 51.3%, $P = 0.082$, see Supplementary Fig. 1).

Voxels in the PoCG mask that were discriminative for task classification and were consistent across at least 6 of 8 subjects over at least 25% RFE selection levels were observed at a typical location for tactile stimulation of the fingers, just posterior to the hand knob area of the contralateral motor cortex (Yousry et al. 1997; Stippich et al. 1999). However, discriminative voxels were not restricted to that region, but extended to more inferior and superior sites of the PoCG. Moreover, even the ipsilateral PoCG showed a contribution to task classification, albeit less pronounced than its contralateral match. The group discrimination map of the PoCG overlapped with BA3b and BA1. These subregions were identified based on the SPM Anatomy toolbox (Geyer et al. 1999, 2000). In addition to these rather early somatosensory regions, voxels in the PPC mask also survived the thresholding criterion for the group discrimination map, that is, in the bilateral supramarginal gyrus, the superior parietal lobule, and the anterior and posterior operculo-insular cortex. The parietal opercular regions covered the somatosensory fields OP1/4 and OP3 and were labeled according to the SPM Anatomy toolbox (Eickhoff, Amunts, et al. 2006; Eickhoff, Schleicher, et al. 2006). In the visual cortex, discriminative voxels were revealed in the posterior calcarine sulcus (pCS) bordering the cuneus and the lateral pOCC and in higher-order regions of the VTC, that is, primarily in the anterior CoS, but also in the FG, the parahippocampal gyrus, and the occipito-temporal sulcus. Finally, voxels discriminating task instructions were also found in the posterior part of the bilateral superior frontal sulcus close to the frontal eye fields and in a left-hemispheric middle frontal gyrus region.

Effects of Perceived Density

Haptic texture exploration trials within the spatial density judgment task were labeled according to individual density ratings. This resulted in 2 trial categories that represented textures that were perceived as either dense or sparse. The classifier performance for density trials exceeded the empirical chance level in 3 of the 6 predefined cortical areas, with 2 of them representing early sensory regions. One of them was the PoCG that showed an average classification performance of 59.1% across subjects (chance level: 52.1%, $P = 0.031$) and the other region was the pOCC that reached a similar above-chance accuracy of 57.3% (chance level: 52.5%, $P = 0.028$). The third cortical site that revealed a significant classifier performance across subjects was the PPC with 59.2% (chance level: 52.1%, $P = 0.012$).

The most discriminative voxels for perceived spatial density classification within the PoCG were located at similar sites as for task classification, including the region opposite to the hand knob area of the motor cortex in both hemispheres. The ipsilateral cluster overlapped with the effect of perceived density identified in the univariate data analysis. There was an additional cluster in the superior PoCG of the contralateral hemisphere and one in the inferior PoCG of the ipsilateral cortex. The group discrimination map in the PoCG overlapped with Brodmann areas 3b and 1, similar to the task discrimination. Voxels that were consistent across at least 6 of 8 subjects over at least 25% RFE selection levels were located in the bilateral pCS extending to the lateral portion of the pOCC. The spatial properties of the group discrimination map in the PoCG and the pOCC resemble the results of the task classification within the same brain regions. However, in contrast to the roughness and density task classification, the discrimination map of trial classification according to perceived spatial density only showed discriminative

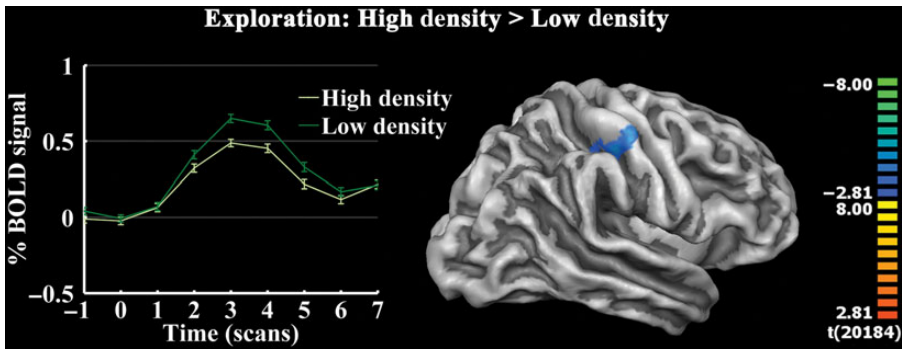

Figure 8. Results of univariate data analysis. The effect of perceived density on a region in the ipsilateral PoCG; *t*-value [Talairach coordinate] of the peak voxel in that cluster: −4.43 [43, −27, 44].

voxels consistent across subjects in the left PPC, contralateral to the exploring hand. These voxels were restricted to the superior parietal lobule and the angular gyrus.

Effects of Perceived Roughness

For the roughness judgment task, haptic exploration trials were labeled according to the individual trial ratings during the fMRI scanning session. We used the trials in the high and low roughness category for classification of the fMRI patterns. Significant above-chance classification of perceived roughness was only found for 2 brain regions, that is, the operculo-insular cortex and the VTC with a mean group accuracy of 57.8% (chance level: 52.2%, $P = 0.020$) and 56.3% (chance level: 52.6%, $P = 0.031$), respectively. None of the other predefined brain areas showed classification performances that were significant across subjects.

Discriminative voxels for roughness classification across subjects were observed bilaterally in posterior and anterior parts of the operculo-insular cortex, not restricted to a specific location, but covering the somatosensory parietal opercular regions OP1 and OP3. This is in contrast to the group discrimination map within the VTC; here, the most discriminative voxels are clearly clustered in the CoS and middle FG of both hemispheres and in the right occipito-temporal sulcus. Although not completely identical, there is some spatial resemblance of the discrimination map for task classification and perceived roughness classification in the VTC.

The results of the task, roughness, and spatial density classification are summarized in Figure 9.

To observe whether the classifier performances for trials differing in perceived roughness or spatial density were not only superior to chance-level performance in the above-identified brain regions, but also significantly different between both texture dimensions, the roughness and spatial density classifier performance was directly compared using an exact permutation test. Hence, for all brain regions that showed an above chance-level classification for different levels of perceived spatial density or roughness, the classification accuracies for both texture dimensions were directly compared across all subjects, indicating a double dissociation in these cortical areas if significant.

Although both spatial density and roughness are dimensions descriptive of texture, we found a double dissociation of cortical regions involved in the processing of these texture dimensions. More specifically, the classifier performance for spatial density exceeded roughness classification in the early occipital and somatosensory cortex as well as in the PPC, whereas the roughness classifier outperformed the density classifier in one higher cortical region, that is, the operculo-insular cortex. Only in the VTC was the direct comparison between both classification results not significant (see Supplementary Fig. 2). Therefore, we wished to verify that the above-chance classification of perceived roughness in the VTC was indeed a direct result of differences in perceived roughness and could not be replicated using another trial labeling procedure. To that end haptic texture exploration trials within the roughness judgment task were labeled according to individual spatial density ratings in the density judgment task. These trials, so labeled, were used for checking the specificity of the classifier performance. Hence, 2 classes were created by grouping stimuli 1.50 and 2.25 mm versus stimuli 5.50 and 8.25 mm in the roughness task. This analysis revealed a nonsignificant classifier performance in the VTC (mean accuracy: 53.1%; chance level: 52.6%; $P = 0.157$).

Effects of Stimulus Spacing

Trial labeling according to stimulus spacing was performed for the haptic exploration intervals in the No-Estimation runs. fMRI patterns were labeled as close spacing when subjects explored textures with interdot distances of 1.50 and 2.25 mm. Trials were grouped to the wide spacing category when subjects touched textures with interdot spacings of 5.50 and 8.25 mm. None of the predefined regions showed average classification accuracies for texture spacing that exceeded the empirical chance level. The average classifier performance across subjects ranged from 51.5% in the PPC to 54.8% in the PoCG, whereas the empirical chance level ranged from 51.8% in the posterior occipital cortex to 52.5% in the PPC (see Supplementary Fig. 3).

Discussion

The current study combined psychophysical and imaging methods to investigate whether the cortical networks underlying density and roughness perception might specifically reflect complexity differences in the mapping between the physical and perceptual space. To this end, fMRI signal patterns elicited by the haptic exploration of dot pattern textures in a roughness and spatial density estimation task were compared. Significant classification accuracies were revealed in all predefined regions, thus confirming previous findings on their involvement in general haptic texture processing. We then went on to investigate whether these same regions hold information about the level of the perceived texture characteristics, that is, the roughness and spatial density rating on each individual trial. In agreement with our hypothesis, we found that information on the perceived spatial density level could be extracted from early sensory cortices, that is, the PoCG (PoCG/CS) and posterior occipital cortex (pOCC), as well as from the PPC, whereas the perceived roughness level could be extracted from higher-order association cortices only, that is, the operculo-insular (OpIns) cortex and the VTC. This result indicates that the cortical texture processing reflects the different complexities of the evaluated haptic texture dimensions, with spatial density information being already available in early sensory regions and information indicative of perceived roughness only in higher-order cortical regions. The pattern of early sensory regions representing simple (spatial density) and higher-order regions more complex texture dimensions (roughness) was not only restricted to the somatosensory regions, but was also present in the classical visual cortex, despite the fact that subjects performed a purely haptic task.

To be able to dissociate spatial density and roughness, we relied on a specific stimulus set for which these perceptual texture dimensions were associated with different psychophysical functions of interelement distance. Overall, the results of the behavioral data analysis corroborate these earlier psychophysical findings with a simple linear relationship of interdot spacing and perceived spatial density and an inverted U-shape function of perceived roughness (Connor et al. 1990; Merabet et al. 2004, 2007; Gescheider et al. 2005; Eck, Kaas, Mulders, et al. 2013; Gescheider and Wright 2013). The psychophysical curve of perceived roughness, however, showed some variation across subjects, in particular the slope of the roughness decrease was affected by interindividual variability. This could be either an effect of the minimally sampled stimulus space in the current study or an effect of subjects having used different rating strategies for wide dot spacing textures. To reduce variability in rating strategies and to ensure an unambiguous roughness categorization of the textures, data from 8 participants with the most consistent and clearly dissociated psychometric curves were included in the fMRI data analysis.

The neuronal correlates of the psychometric curves were investigated using uni- and multivariate approaches. The latter

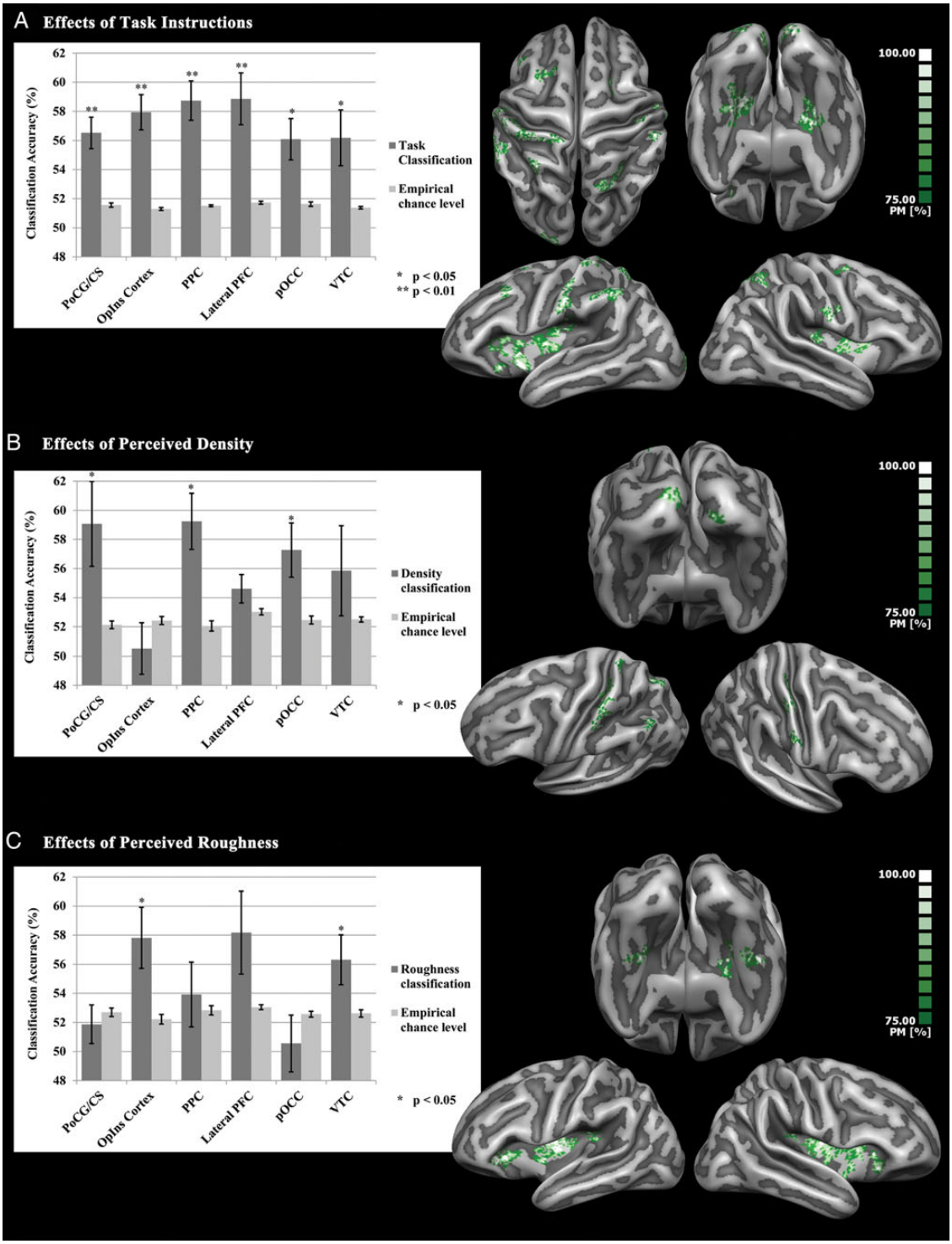

Figure 9. Results of multivariate data analysis. The left side of the figure shows the average classification accuracies across all subjects together with the average permutation accuracies for all predefined regions; the bars represent the standard error of the mean (SEM). In the right panel, group discrimination maps are presented on the average cortex reconstruction of all subjects. The color-coding of the vertices represents the consistency across subjects within the different predefined regions. Green-colored voxels outlasted at least 25% of the RFE selection steps in at least 6 of 8 subjects (75%), whereas white-colored voxels survived in all subjects (100%).

provided the high sensitivity needed to detect the small signal changes expected for a task with similar sensory input, but a change in perceptual focus. The univariate analysis of the neuroimaging data revealed a significant effect of perceived spatial density in the right but not in the left postcentral cortex. This result is unexpected considering that subjects performed the task with their right hand. However, an event-related averaging analysis in that region clearly showed that this effect was not due to

signal differences below the baseline level. Furthermore, although not as common in the literature as contralateral activation changes, effects in ipsilateral postcentral regions have been reported before for tactile tasks, as for example by Debowska et al. (2013); van Ede et al. (2014), and Sathian et al. (2013). More specifically, studies focusing on macrospatial tasks, such as orientation and shape discrimination, showed activation within the right PoCS and the neighboring intraparietal sulcus, irrespective of the hand used for tactile exploration (Kitada et al. 2006; Stilla and Sathian 2008), the same is true for studies using microspatial discrimination tasks (Sathian et al. 2013). These studies, together with our results, indicate a right-hemispheric contribution to aspects of tactile spatial coding. Interestingly, there was neither an effect of perceived roughness nor of task instructions (roughness vs. density estimation) in the univariate data analysis.

In contrast to the univariate approach, the multivariate analysis of the same data revealed effects of task instructions, perceived spatial density and roughness, indicating that multivariate techniques are indeed more sensitive to subtle differences in the activation patterns of haptic tasks. This increased sensitivity might also have the unwanted side effect of capturing subtle differences which are not necessarily of interest, for example, effects of different haptic exploration strategies or motion artifacts. Precautionary measures were taken to minimize these problems. The exact haptic exploration movement was predefined and all participants were exhaustively trained in the mock scanner before entering the fMRI experiment. Furthermore, the same experimenter was responsible for stimulus presentation in all subjects and indicated with a separate button box, whether a participant missed a trial or the exploration movement was not correctly timed or incorrect. These trials were removed from data analysis. In addition, we used the motion parameters and task regressors from the univariate analysis to check for correlations of the model with motion effects (see Supplementary Fig. 4). The results were unsuspicious and indicated that motion was not a significant contributor to the multivariate results in this study.

All ROIs showed significant above-chance classification of the estimation tasks across subjects, whereas the same classification was not significant in a control region, that is, Heschl's gyrus, indicating the validity of the results for the selected ROIs. Notably, there was neither a difference in the employed texture set nor in the experimental design of both rating tasks; the only difference was the task instruction for the subjects. Hence, early sensory regions including the PoCG/CS and the pOCC as well as higher-order areas, such as the lateral PFC, the OpIns cortex, the PPC, and the VTC, convey information indicative of the performed haptic texture task. The effect of task in the somatosensory cortex was not restricted to but included the cortical input regions for cutaneous information (Kaas 1993), that is, BA3b constituting the SI and BA1 as a projection site of BA3b. Furthermore, the involvement of OP1/4 and OP3 in task classification supports earlier findings, indicating an involvement of these somatosensory parietal opercular fields in texture perception (Stilla and Sathian 2008; Sathian et al. 2011). Interestingly, significant classification effects were not restricted to somatosensory regions and the prefrontal cortex, which would be expected from a purely tactile task. Classical visual regions in the posterior occipital cortex and the VTC showed a similar pattern for task classification. This is consistent with the current body of haptic literature, which shows an involvement of visual cortex regions in tactile tasks (Sathian et al. 1997, 2011; Amedi et al. 2001; Stoesz et al. 2003; Merabet et al. 2007; Peltier et al. 2007; Deshpande et al. 2008; Podrebarac et al. 2014).

Based on the task classification, we cannot infer which of these regions are involved in spatial density estimation of the dot pattern textures and which contribute to roughness perception. To that end we tested whether some of these regions also hold information that discriminates texture trials that were perceived by the participants as either rough/dense or smooth/sparse. In agreement with earlier studies, we found significant above-chance classification of the spatial density classes in early somatosensory (Zangaladze et al. 1999; Merabet et al. 2007) and visual cortex (Merabet et al. 2004), but also in 2 higher parietal regions, namely the left superior parietal lobule and the angular gyrus.

Interestingly though, SVM classification of *physical* wide and close interdot spacing in the No-Estimation runs did not exceed the empirical chance level in the same regions. At first sight, this is somewhat surprising considering that texture categorization according to physical interdot spacing was identical to categorization according to perceived spatial density, as indicated by the simple negative linear relationship of the physical and perceptual texture characteristic, observed in the behavioral results. It is possible that a classification above-chance level could have been reached by increasing the power, that is, the number of stimulus repetitions. The lack of significant findings from the No-Estimation runs cannot be explained by different sensory input, as we can be certain that all participants reliably performed identical haptic exploration of the stimuli in all runs. Hence, a more likely cause of the lack of significant findings is the absence of an explicit judgment task, which might have resulted in a redirection of the participants' attention elsewhere. In the same vein, the significant density classifications in the Rating runs could be explained by the enhanced attention to the physical stimulus space, induced by the rating instruction, which might have promoted the cortical processing of small differences in the tactile texture set. Such top-down influences on tactile stimulus processing have been observed as early as in the S1 (Sterr et al. 2007; van Ede et al. 2014) and are also well known for visual processing (Treue 2001; Andersen et al. 2008). Furthermore, the involvement of the posterior occipital cortex in a mere tactile task is in agreement with the idea that primary sensory regions share similar representations, an idea suggested by Merabet et al. (2004) and further elaborated by Eck, Kaas, Goebel (2013). In summary, the results of the perceived spatial density and physical spacing SVM classification indicate that differences in the physical stimulus space of tactile textures are represented in early sensory regions of the visual and the somatosensory cortex as well as in higher parietal areas, but that attention to the perceptual texture dimension is necessary to reveal this information.

In contrast to perceived spatial density, perceived roughness information appears to be conveyed predominantly by higher-order cortical areas as indicated by classifications above the empirical chance level in the operculo-insular cortex and the VTC. The parietal opercular regions included OP1, the homolog of SII (Eickhoff, Amunts, et al. 2006), and OP3, both of which have previously been implicated in roughness perception (Kitada et al. 2005; Burton et al. 2008; Simões-Franklin et al. 2011). The significant findings in higher-order regions could be interpreted as support of our hypothesis that perceived roughness requires an integration of multiple factors likely to be represented in association cortex. The lack of significant findings in early sensory cortices could point to an insufficient sensitivity of our experimental design to reveal roughness-related signal changes in these regions, as it was previously shown that neuronal activity in monkey S1 codes for texture differences that represented differences in perceived roughness (Sinclair and Burton 1991; Jiang

et al. 1997). However, these experiments employed stimuli in which either the groove width of linear gratings or the interdot spacing of dot patterns fell in a range where they are expected to be approximately linearly related to perceived roughness (Meftah et al. 2000; Lawrence et al. 2007). Hence, the confounded spatial and roughness characteristics of the stimuli render it almost impossible to answer the question which texture property is eventually coded by the neuronal cells in S1. Nevertheless, this does not exclude the possibility that roughness differences are indeed represented in the primary sensory cortex, but that our experimental design was not sensitive enough to pick up these differences.

In addition to the significant classification of perceived roughness categories in the operculo-insular cortex, the same was found for the VTC. A direct comparison of the roughness and spatial density classifier did not reveal a better performance for roughness differences. However, the spatial density classifier did not exceed empirical chance level in the VTC. Moreover, classification of roughness trials based on spatial density ratings yielded chance classification. Although not completely conclusive, this result provides a first indication that the VTC contains information indicative of tactile texture roughness. The most discriminative voxels in the CoS for high and low roughness classification were close to fMRI activation peaks previously reported for visual attention to surface textures (Cant and Goodale 2007; Cant and Xu 2012). This would be expected as the VTC region in our study was defined based on a visual texture localizer. However, a recent study showed that a similar region is insensitive to low-level changes such as in density or spacing, but responds to changes in high-level information, such as differences in the ratio of 2 types of objects in an ensemble (Cant and Xu 2014). This result is in accordance with the view that complex high-level perceptual information is represented in the VTC, while image-based low-level properties are processed in early visual regions (Hiramatsu et al. 2011; Goda et al. 2014). Interestingly, in our study, we found indications that the VTC conveys perceptual information based on tactile input. Specifically, it contained information on perceived roughness, a more complex texture dimension when compared with perceived spatial density. A general contribution of the occipital and temporal cortex to a tactile roughness categorization task was also reported by Simões-Franklin et al. (2011).

Analogous to the primary somatosensory and visual cortex sharing a representation of low-level perceptual texture dimensions such as spatial density, the operculo-insular cortex, and VTC could share a representation of complex or high-level texture dimensions such as perceived roughness. Both the visual and the somatosensory components of the network might be invoked either visually or haptically via learned associations of visuo-tactile texture perception.

We cannot be certain whether our results can be generalized to other kinds of textures. Sutu et al. (2013), for example, reported a linear increase in perceived roughness with increasing interdot spacing, using very similar dot patterns but with slightly higher dots. The authors suggested that a simple intensive code (mean discharge rate of primary mechanoreceptive afferents) might explain these roughness-related changes. Furthermore, they argued that this interpretation is supported by the finding that neuronal discharge rates in monkey S1 increase over a similar range as roughness perception did in their experiment (Jiang et al. 1997). Although this is an interesting conjecture, to our knowledge, no neuroimaging study has been published so far reporting roughness-related changes in the human S1. In contrast to the higher dot pattern textures, Sutu et al. (2013) found a comparable inverted U-shape function as we did when testing roughness perception on dot pattern stimuli with lower dots. They interpreted this finding as an indication that subjects judged texture roughness for the ascending limb of the inverted U function, but some other texture quality for the descending limb. However, the consistency of roughness-related activation changes in the human operculo-insular cortex in our and other studies using different textures, that is, sandpaper and linear gratings (Kitada et al. 2005; Simões-Franklin et al. 2011), leads us to believe that our subjects indeed judged roughness, all the more because these studies also found no roughness-related changes in the S1. This consistency with other studies using different texture sets corroborates our findings of roughness-related changes in the operculo-insular cortex and the VTC.

In summary, we found that both early and higher-order visual, somatosensory, and prefrontal regions conveyed information indicative of the tactile task performed on an identical set of textures, that is, judging spatial density versus roughness. However, while different levels of perceived spatial density could already be decoded from fMRI activation patterns in early sensory but also in higher somatosensory association cortices, information on the perceived roughness level was solely available in higher-order regions of the ventral visual cortex and the operculo-insular cortex. These cortical differences appear to corroborate the psychophysical findings, implicating that perceived spatial density represents a simple mapping of the physical stimulus space, whereas perceived roughness is influenced by multiple factors. These results confirm and also extend earlier reports by showing that the visual cortex is not only involved in judging spatial characteristics of tactile textures, but also contributes to tactile roughness perception.

A possible interpretation of the findings includes a shared representation of perceived texture characteristics in somatosensory and visual cortices, with spatial density relying on early sensory regions and roughness on higher-order sensory cortices, which might be accessible via both sensory modalities through learned associations in visuo-tactile texture perception.

Supplementary Material

Supplementary material can be found at: http://www.cercor.oxfordjournals.org/.

Funding

This work was supported by the European Community's Seventh Framework Programme FP7/2007-2013 (PITN-GA-2008-214728) and the BrainGain Smart Mix Programme of the Netherlands Ministry of Economic Affairs and the Netherlands Ministry of Education, Culture and Science (SSM06011).

Notes

We thank Alan Meeson and Giancarlo Valente for their very helpful remarks on the data analysis, Valerie Goffaux for her great help with designing the visual texture localizer, and Emma Biggs for her valuable comments on the manuscript. *Conflict of Interest*: None declared.

References

Amedi A, Malach R, Hendler T, Peled S, Zohary E. 2001. Visuo-haptic object-related activation in the ventral visual pathway. Nat Neurosci. 4:324–330.

Andersen SK, Hillyard SA, Muller MM. 2008. Attention facilitates multiple stimulus features in parallel in human visual cortex. Curr Biol. 18:1006–1009.

Bergmann Tiest WM. 2010. Tactual perception of material properties. Vision Res. 50:2775–2782.

Bergmann Tiest WM, Kappers AML. 2006. Analysis of haptic perception of materials by multidimensional scaling and physical measurements of roughness and compressibility. Acta Psychol (Amst). 121:1–20.

Bergmann Tiest WM, Kappers AML. 2007. Haptic and visual perception of roughness. Acta Psychol (Amst). 124:177–189.

Blake DT, Hsiao SS, Johnson KO. 1997. Neural coding mechanisms in tactile pattern recognition: the relative contributions of slowly and rapidly adapting mechanoreceptors to perceived roughness. J Neurosci. 17:7480–7489.

Burton H, Sinclair RJ, Wingert JR, Dierker DL. 2008. Multiple parietal operculum subdivisions in humans: tactile activation maps. Somatosens Mot Res. 25:149–162.

Cant JS, Goodale MA. 2007. Attention to form or surface properties modulates different regions of human occipitotemporal cortex. Cereb Cortex. 17:713–731.

Cant JS, Xu Y. 2015. The impact of density and ratio on object-ensemble representation in human anterior-medial ventral visual cortex. Cereb Cortex. 25:4226–4239.

Cant JS, Xu Y. 2012. Object ensemble processing in human anterior–medial ventral visual cortex. J Neurosci. 32:7685–7700.

Connor CE, Hsiao SS, Phillips JR, Johnson KO. 1990. Tactile roughness: neural codes that account for psychophysical magnitude estimates. J Neurosci. 10:3823–3836.

Culham JC, Valyear KF. 2006. Human parietal cortex in action. Curr Opin Neurobiol. 16:205–212.

Debowska W, Wolak T, Soluch P, Orzechowski M, Kossut M. 2013. Design and evaluation of an innovative MRI-compatible Braille stimulator with high spatial and temporal resolution. J Neurosci Methods. 213:32–38.

De Martino F, Valente G, Staeren N, Ashburner J, Goebel R, Formisano E. 2008. Combining multivariate voxel selection and support vector machines for mapping and classification of fMRI spatial patterns. Neuroimage. 43:44–58.

Dépeault A, Meftah E-M, Chapman C. 2009. Tactile perception of roughness: raised-dot spacing, density and disposition. Exp Brain Res. 197:235–244.

Deshpande G, Hu X, Stilla R, Sathian K. 2008. Effective connectivity during haptic perception: a study using Granger causality analysis of functional magnetic resonance imaging data. Neuroimage. 40:1807–1814.

Eck J, Kaas AL, Goebel R. 2013. Crossmodal interactions of haptic and visual texture information in early sensory cortex. Neuroimage. 75:123–135.

Eck J, Kaas AL, Mulders JL, Goebel R. 2013. Roughness perception of unfamiliar dot pattern textures. Acta Psychol (Amst). 143:20–34.

Eickhoff SB, Amunts K, Mohlberg H, Zilles K. 2006. The human parietal operculum. II. Stereotaxic maps and correlation with functional imaging results. Cereb Cortex. 16:268–279.

Eickhoff SB, Grefkes C, Fink GR, Zilles K. 2008. Functional lateralization of face, hand, and trunk representation in anatomically defined human somatosensory areas. Cereb Cortex. 18: 2820–2830.

Eickhoff SB, Grefkes C, Zilles K, Fink GR. 2007. The somatotopic organization of cytoarchitectonic areas on the human parietal operculum. Cereb Cortex. 17:1800–1811.

Eickhoff SB, Schleicher A, Zilles K, Amunts K. 2006. The human parietal operculum. I. Cytoarchitectonic mapping of subdivisions. Cereb Cortex. 16:254–267.

Forman SD, Cohen JD, Fitzgerald M, Eddy WF, Mintun MA, Noll DC. 1995. Improved assessment of significant activation in functional magnetic resonance imaging (fMRI): use of a cluster-size threshold. Magn Reson Med. 33:636–647.

Frost MA, Goebel R. 2012. Measuring structural-functional correspondence: spatial variability of specialised brain regions after macro-anatomical alignment. Neuroimage. 59:1369–1381.

Gescheider GA, Bolanowski SJ, Greenfield TC, Brunette KE. 2005. Perception of the tactile texture of raised–dot patterns: a multidimensional analysis. Somatosens Mot Res. 22:127–140.

Gescheider GA, Wright JH. 2013. Roughness perception in tactile channels: evidence for an opponent process in the sense of touch. Somatosens Mot Res. 30:120–132.

Geyer S, Schleicher A, Zilles K. 1999. Areas 3a, 3b, and 1 of human primary somatosensory cortex. Neuroimage. 10:63–83.

Geyer S, Schormann T, Mohlberg H, Zilles K. 2000. Areas 3a, 3b, and 1 of human primary somatosensory cortex. Part 2. Spatial normalization to standard anatomical space. Neuroimage. 11:684–696.

Goda N, Tachibana A, Okazawa G, Komatsu H. 2014. Representation of the material properties of objects in the visual cortex of nonhuman primates. J Neurosci. 34:2660–2673.

Goebel R, Esposito F, Formisano E. 2006. Analysis of functional image analysis contest (FIAC) data with brainvoyager QX: from single-subject to cortically aligned group general linear model analysis and self-organizing group independent component analysis. Hum Brain Mapp. 27:392–401.

Goulas A, Uylings HBM, Stiers P. 2012. Unravelling the intrinsic functional organization of the human lateral frontal cortex: a parcellation scheme based on resting state fMRI. J Neurosci. 32:10238–10252.

Hiramatsu C, Goda N, Komatsu H. 2011. Transformation from image-based to perceptual representation of materials along the human ventral visual pathway. Neuroimage. 57:482–494.

Hollins M, Bensmaia S, Karlof K, Young F. 2000. Individual differences in perceptual space for tactile textures: evidence from multidimensional scaling. Percept Psychophys. 62:1534–1544.

Hollins M, Faldowski R, Rao S, Young F. 1993. Perceptual dimensions of tactile surface texture: a multidimensional scaling analysis. Percept Psychophys. 54:697–705.

Jiang W, Tremblay F, Chapman CE. 1997. Neuronal encoding of texture changes in the primary and the secondary somatosensory cortical areas of monkeys during passive texture discrimination. J Neurophysiol. 77:1656–1662.

Johnson KO. 2001. The roles and functions of cutaneous mechanoreceptors. Curr Opin Neurobiol. 11:455–461.

Kaas JH. 1993. The functional organization of somatosensory cortex in primates. Ann Anat. 175:509–518.

Kitada R, Hashimoto T, Kochiyama T, Kito T, Okada T, Matsumura M, Lederman SJ, Sadato N. 2005. Tactile estimation of the roughness of gratings yields a graded response in the human brain: an fMRI study. Neuroimage. 25:90–100.

Kitada R, Kito T, Saito DN, Kochiyama T, Matsumura M, Sadato N, Lederman SJ. 2006. Multisensory activation of the intraparietal area when classifying grating orientation: a functional magnetic resonance imaging study. J Neurosci. 26:7491–7501.

Lawrence MA, Kitada R, Klatzky RL, Lederman SJ. 2007. Haptic roughness perception of linear gratings via bare finger or rigid probe. Perception. 36:547–557.

Ledberg A, O'Sullivan BT, Kinomura S, Roland PE. 1995. Somatosensory activations of the parietal operculum of man. A PET study. Eur J Neurosci. 7:1934–1941.

Lederman SJ, Taylor MM. 1972. Fingertip force, surface geometry, and the perception of roughness by active touch. Percept Psychophys. 12:401–408.

Lederman SJ, Thorne G, Jones B. 1986. Perception of texture by vision and touch: multidimensionality and intersensory integration. J Exp Psychol Hum Percept Perform. 12:169–180.

Mazzola L, Faillenot I, Barral FG, Mauguiere F, Peyron R. 2012. Spatial segregation of somato-sensory and pain activations in the human operculo-insular cortex. Neuroimage. 60:409–418.

Meftah EM, Belingard L, Chapman CE. 2000. Relative effects of the spatial and temporal characteristics of scanned surfaces on human perception of tactile roughness using passive touch. Exp Brain Res. 132:351–361.

Merabet L, Thut G, Murray B, Andrews J, Hsiao S, Pascual-Leone A. 2004. Feeling by sight or seeing by touch? Neuron. 42:173–179.

Merabet LB, Swisher JD, McMains SA, Halko MA, Amedi A, Pascual-Leone A, Somers DC. 2007. Combined activation and deactivation of visual cortex during tactile sensory processing. J Neurophysiol. 97:1633–1641.

O'Sullivan BT, Roland PE, Kawashima R. 1994. A PET study of somatosensory discrimination in man. microgeometry versus macrogeometry. Eur J Neurosci. 6:137–148.

Peltier S, Stilla R, Mariola E, LaConte S, Hu X, Sathian K. 2007. Activity and effective connectivity of parietal and occipital cortical regions during haptic shape perception. Neuropsychologia. 45:476–483.

Picard D, Dacremont C, Valentin D, Giboreau A. 2003. Perceptual dimensions of tactile textures. Acta Psychol (Amst). 114:165–184.

Podrebarac SK, Goodale MA, Snow JC. 2014. Are visual texture-selective areas recruited during haptic texture discrimination? Neuroimage. 94C:129–137.

Roland PE, O'Sullivan B, Kawashima R. 1998. Shape and roughness activate different somatosensory areas in the human brain. Proc Natl Acad Sci USA. 95:3295–3300.

Sanchez-Panchuelo RM, Francis S, Bowtell R, Schluppeck D. 2010. Mapping human somatosensory cortex in individual subjects with 7T functional MRI. J Neurophysiol. 103:2544–2556.

Sathian K, Deshpande G, Stilla R. 2013. Neural changes with tactile learning reflect decision-level reweighting of perceptual readout. J Neurosci. 33:5387–5398.

Sathian K, Lacey S, Stilla R, Gibson GO, Deshpande G, Hu X, LaConte S, Glielmi C. 2011. Dual pathways for haptic and visual perception of spatial and texture information. Neuroimage. 57:462–475.

Sathian K, Zangaladze A, Hoffman JM, Grafton ST. 1997. Feeling with the mind's eye. Neuroreport. 8:3877–3881.

Simões-Franklin C, Whitaker TA, Newell FN. 2011. Active and passive touch differentially activate somatosensory cortex in texture perception. Hum Brain Mapp. 32:1067–1080.

Sinclair RJ, Burton H. 1991. Neuronal activity in the primary somatosensory cortex in monkeys (*Macaca mulatta*) during active touch of textured surface gratings: responses to groove width, applied force, and velocity of motion. J Neurophysiol. 66:153–169.

Sterr A, Shen S, Zaman A, Roberts N, Szameitat A. 2007. Activation of SI is modulated by attention: a random effects fMRI study using mechanical stimuli. Neuroreport. 18:607–611.

Stilla R, Sathian K. 2008. Selective visuo-haptic processing of shape and texture. Hum Brain Mapp. 29:1123–1138.

Stippich C, Hofmann R, Kapfer D, Hempel E, Heiland S, Jansen O, Sartor K. 1999. Somatotopic mapping of the human primary somatosensory cortex by fully automated tactile stimulation using functional magnetic resonance imaging. Neurosci Lett. 277:25–28.

Stoesz MR, Zhang M, Weisser VD, Prather SC, Mao H, Sathian K. 2003. Neural networks active during tactile form perception: common and differential activity during macrospatial and microspatial tasks. Int J Psychophysiol. 50:41–49.

Stringer EA, Chen LM, Friedman RM, Gatenby C, Gore JC. 2011. Differentiation of somatosensory cortices by high-resolution fMRI at 7 T. Neuroimage. 54:1012–1020.

Sutu A, Meftah el M, Chapman CE. 2013. Physical determinants of the shape of the psychophysical curve relating tactile roughness to raised-dot spacing: implications for neuronal coding of roughness. J Neurophysiol. 109:1403–1415.

Suykens JAK, De Brabanter J, Lukas L, Vandewalle J. 2002. Weighted least squares support vector machines: robustness and sparse approximation. Neurocomputing. 48:85–105.

Treue S. 2001. Neural correlates of attention in primate visual cortex. Trends Neurosci. 24:295–300.

van Ede F, de Lange FP, Maris E. 2014. Anticipation increases tactile stimulus processing in the ipsilateral primary somatosensory cortex. Cereb Cortex. 24:2562–2571.

Weber AI, Saal HP, Lieber JD, Cheng JW, Manfredi LR, Dammann JF III, Bensmaia SJ. 2013. Spatial and temporal codes mediate the tactile perception of natural textures. Proc Natl Acad Sci USA. 110:17107–17112.

Yousry TA, Schmid UD, Alkadhi H, Schmidt D, Peraud A, Buettner A, Winkler P. 1997. Localization of the motor hand area to a knob on the precentral gyrus. A new landmark. Brain. 120(Pt 1):141–157.

Zangaladze A, Epstein CM, Grafton ST, Sathian K. 1999. Involvement of visual cortex in tactile discrimination of orientation. Nature. 401:587–590.